An experimental study of Ge diffusion through Ge2Sb2Te5

Minh Anh Luong, Sijia Ran, Mathieu Bernard, Alain Claverie

An Experimental Study of Ge Diffusion through $Ge_2Sb_2Te_5$

Minh Anh Luong[1]*, Sijia Ran[1], Mathieu Bernard[2] and Alain Claverie[1]*

[1] CEMES-CNRS, 29 Rue Jeanne Marvig, 31055 Toulouse, France.
[2] Léti-CEA, 17 Avenue des Martyrs, F-38000 Grenoble, France

Corresponding authors: minh-anh.luong@cemes.fr, claverie@cemes.fr

Abstract:

Ge thermal diffusion is not only the phenomenon limiting the decomposition and crystallization of Ge-rich GeSbTe alloys but is also responsible for some of the failures of the phase change memory devices using them. However, Ge diffusion in the canonical $Ge_2Sb_2Te_5$ (GST-225) or in Ge-rich GeSbTe (GGST) alloys has been little studied experimentally. For these reasons, we have designed and set up a series of experiments aimed at highlighting and studying this diffusion within the solid phase, under technologically relevant conditions. For that, dedicated GST/Ge/GST structures have been grown at purpose, and the redistribution of Ge in GST-225 layers during isothermal and isochronal annealing has been studied using scanning and transmission electron microscopy based techniques. While Ge diffusion in amorphous GST-225 is negligible at low temperatures (i.e., below 140°C), it is fast in crystalline GST-225 above 220°C and proceeds via the grain boundaries. During such annealing, Ge diffusion is only limited by the emission of Ge atoms from the solid source and by the density of the grain boundaries providing diffusion paths to Ge through the polycrystalline layer, which tends to decrease as a function of the annealing time as the GST grains coalesce. These results show that diffusion phenomena can be activated at moderate temperatures in GST alloys and can change the chemical composition and morphology of Ge/GST composite materials. This supports the hypothesis that Ge diffusion may be responsible for the observed resistance drift and loss of integrity of the Phase Change Memories based on Ge-rich GeSbTe alloys in the SET state.

1. Introduction and Motivation

Phase-Change Memories (PCMs) offer a number of characteristics which make them suitable to replace and extend the range of applications of the current non-volatile electronic memories. [1–5] Beyond the possibility to scale them down and integrate them into large arrays, they show impressive data retention and endurance characteristics. [6,7] The working principle of digital PCMs relies on the phase transition between an amorphous (high resistivity) state and a crystalline (low resistivity) state, which can then be associated to the binary states of an electronic memory. Switching from one state to the other is obtained by heating of a dome of a few tens nanometers in diameter with appropriate current pulses able to locally melt then quench the material or, alternatively, recrystallize it. Furthermore, intermediate resistance states can be programmed in such memory nodes so that multilevel data storage concepts are thinkable, using PCMs. [8–10] The canonical alloy $Ge_2Sb_2Te_5$ (GST-225) is the most widely used active material in PCM cells. However, it is often doped with other elements to enhance the device performances. Automotive and smart card applications, for example, require alloys offering a higher thermal stability, i.e. a crystallization temperature (Tx) higher than that of GST-225 (about 170°C). This is why Ge-rich GST (GGST) alloys which offer Tx as high as 300-350°C are receiving today increasing attention. [11–15]

Different from GST-225, a congruent material which keeps a homogeneous chemical composition during phase transition, amorphous Ge-rich GST alloys (GGST) decompose during thermal annealing, and the materials ultimately crystallize by forming a mixture of Ge and GST-225 grains. [13,14,16] The crystallization kinetics, and by extension the speed of the SET operation of the PCM device, will be limited by the rate at which Ge separates from the GST alloys, i.e. on Ge diffusivity in this amorphous glass. Moreover, a number of failures affecting the characteristics of PCM devices based on GST alloys can be attributed to segregation phenomena of the chemical elements constituting these alloys or to the inhomogeneities in the stoichiometry of the phases in presence. This is the case of the "RESET stuck" of GST-225-based PCMs and of the "SET and RESET stuck" affecting GGST-based PCMs. [17–19] In both cases, it is strongly suspected that the repetition of sequences , i.e. “melt-quench-recrystallization” (of the order of 10^{11} RESET/SET cycles), results in the separation of chemical species in and around the dome region of the cell. These dynamic melting and quenching effects depend on the diffusivity of the chemical species within the PCM cells, in the liquid and super-cooled liquid phases. Another phenomenon probably involves Ge diffusivity: the SET drift observed in GGST cells, partly minimised by the nitrogen doping.[11,20,21] It is commonly accepted that these variations in resistivity observed at temperatures ranging from room temperature to some 200°C result from Ge diffusion via these grain boundaries and from the subsequent atomic rearrangements at the grain boundaries.[18,22,23]

In summary, several types of diffusivity would be needed to describe and simulate the atomic mechanisms involved in the forming, SET and RESET operations of PCM cells, as well as to predict the observed degradations (drifts or failures) of PCM cells based on GST alloys, over time. Unfortunately, the literature is poor in data relevant to the diffusion of Ge in GST alloys.

Table 1 summarises the values of the diffusion coefficients of Ge, Sb and Te in GST-225 alloy that can be gathered in literature.

Authors	Method	Phase	T (°C)	Diffusion coefficient ($cm^2\ s^{-1}$)	Ref
Privitera et al.	Laser irradiated and COMSOL calculations	Molten phase	627	$D_{Ge/GST}$ = 2 to 8x10^{-5}	Ref[24]
Akola et al.	Density functional calculations	Molten phase	627	$D_{Ge/GST} = 3.93 \times 10^{-5}$	Ref[25]
				$D_{Sb/GST} = 4.67 \times 10^{-5}$	
				$D_{Te/GST} = 3.78 \times 10^{-5}$	
Li et al.	ab initio molecular dynamics simulations	Crystalline	327	$D_{Ge/GST} = 5.17 \times 10^{-6}$	Ref[26]
				$D_{Sb/GST} = 4.28 \times 10^{-6}$	
				$D_{Te/GST} = 2.35 \times 10^{-6}$	
Shen et al.	ab initio molecular dynamics simulations	Crystalline	327	$D_{Ge/GST} = 1.16 \times 10^{-6}$	Ref[27]
				$D_{Sb/GST} = 1.5 \times 10^{-6}$	
				$D_{Te/GST} = 1.18 \times 10^{-6}$	
Novielli et al.	Finite element method	Molten	620-887	Diffusivity 10^{-5} to 10^{-4}	Ref[28]
		Crystalline	410-620	Diffusivity 10^{-9} to 10^{-7}	
		Amorphous/ Crystalline	113-410	Diffusivity 10^{-12} to 10^{-9}	

***Table 1**: Ge-Sb-Te diffusivity values reported in literature.*

Firstly, we note that only one publication (Privitera et al. [24]) reports an (indirect) experimental estimate of the diffusivity of Ge, and only in the liquid phase. The reason for this lack of experimental results is largely due to the difficulty of evidencing and measuring the diffusion of a species within a matrix already containing at least 22% of this element. Only significant variations in composition can then be experimentally detected. On the other hand, the design and fabrication of dedicated structures and the implementation of relevant methodologies to measure, over time and as a function of temperature, the diffusion of Ge in a GST matrix are not trivial. Most of the available data therefore come from theoretical work obtained by various approaches, at fairly variable temperatures. For example, Li et al. [26] and Shen et al. [27] calculated the diffusivity of Ge in monocrystalline GST-225 at 327°C. Li obtained a slightly higher diffusivity of Sb than Ge and Te. Privitera et al. [24] and Akola et al. [25] calculated the diffusivity of Ge in the liquid phase. Their results are consistent and in agreement with the experimental estimate and again show a slightly higher diffusivity of Sb, compared to Ge and Te. Finally, Novielli et al. [28] have extracted values of these diffusivities after calibration of a model describing the segregation of species in PCM cells. The analysis of these publications shows that while the diffusivity of Ge is relatively well documented in the liquid phase, the quantities necessary for the simulation of a number of technological situations are non-existent.

2. Experimental Challenge and Approach

Figure 1 shows the structural and chemical characteristics of a typical GGST-based PCM cell in the RESET, i.e. in its highly resistive, state. While the region far from the cell is composed of a mixture of Ge and GST-225 grains, the dome cell region is characterised by an almost pure Ge "crown" surrounding an amorphous dome much poorer in Ge than the initial GGST alloy. These compositional heterogeneities are then found, more or less pronounced, in the SET and RESET states and are characteristics of PCM cells based on GGST alloys. [13,14,16]

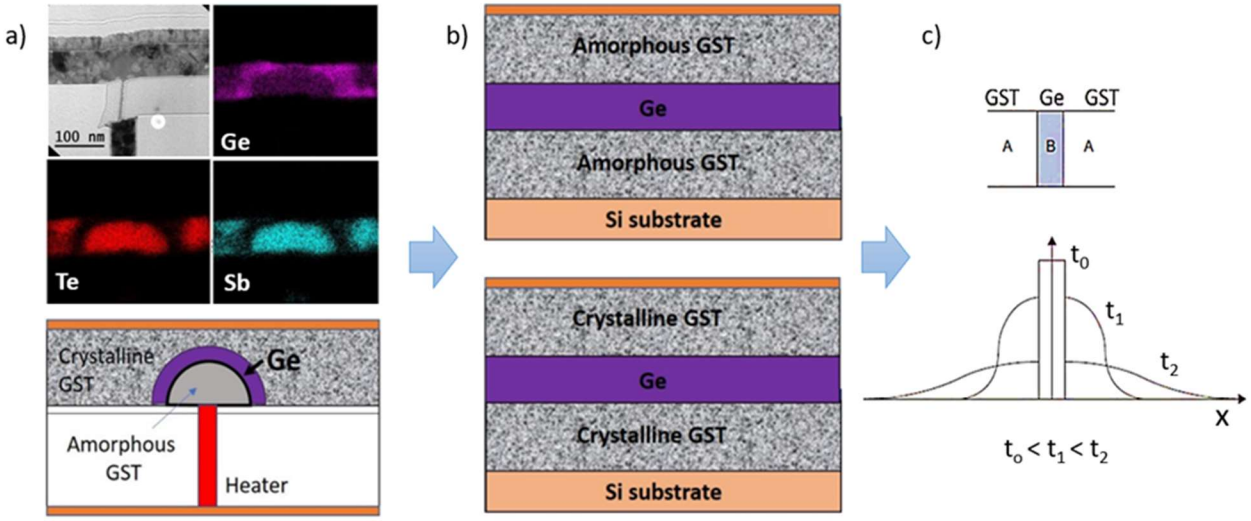

***Figure 1**: a) Transmission electron microscopy (TEM) image, chemical maps and schematic illustration evidencing the typical structure and chemical distributions of Ge-Sb-Te within a GGSTN cell after the forming operation. b) scheme showing the planar sandwiched structure reproducing the interfaces of interest in a GGST cell. c) Top, classical structure used to study the diffusion of an impurity into a solid from an infinite source. Bottom, chemical profiles classically observed during diffusion experiments.*

Describing the crystallization of the amorphous dome, i.e. the SET operation and, beyond that, the thermal stability of the SET and RESET states, would require the ability to describe the diffusive behaviour of Ge in contact with and inside the GST material, both in the amorphous and polycrystalline phases. However, studying this kinetic phenomenon at this spatial scale is inaccessible. For these reasons, we have attempted to reproduce, by "planarizing" it, the situation encountered in a PCM dome cell structure in order to study in detail the behaviour, during thermal annealing, of a Ge layer in contact with a GST-225 layer, either amorphous or crystalline, as shown in Fig. 1. The structure we propose (Fig. 1b) not only allows us to "mimic" the situation encountered within a cell, but also to perform, in principle, a classical diffusion experiment from a solid source (Fig. 1c). In such an experiment, the atoms constituting the source (B) diffuse within the layers (A) and show concentration profiles as a function of distance from the source that evolve over time, typical of the diffusion mechanism activated at the temperature considered. The laws of diffusion and some mathematical manipulations allow, in principle, to deduce the diffusion coefficient at a given temperature from the fitting of concentration profiles measured over time by simple mathematical functions. [29–31] As diffusion is thermally activated, the measurement of diffusion coefficients obtained at different temperatures can then be used to establish a general expression for the diffusivity of the species under study. However, as it will be emphasized later, such an approach is restricted to the usual cases where the solid has a thickness larger than the diffusion length.

We have therefore fabricated such structures by physical deposition on a thermally oxidized 200 mm Si wafer. A 50 nm-thick amorphous Ge "source" layer was buried between two 115 nm thick

amorphous GST-225 layers. This GST/Ge/GST stack was deposited at room temperature in an Ar atmosphere by magnetron sputtering on a Si(100) wafer of 200 mm diameter in an ultra-high vacuum industrial tool (EVATEC ClusterLine200TM) by alternating sputtering of a $Ge_2Sb_2Te_5$ target and of a pure Ge target. Films were deposited on Si substrates previously cleaned by Ar sputtering. The stack was protected against oxidation by depositing in situ, immediately after fabrication, a 10 nm thick SiN capping layer. Annealing experiments were performed either in situ in a TEM, following a procedure minimizing experimental artefacts, as presented in detail by Luong et al. [32], or ex situ, in a conventional annealing furnace, under nitrogen flux. XRD measurements were carried out using a Bruker D8 Discover diffractometer with a Cu - Ka1 source (λ = 1.5406 Å). Thin specimens suitable for cross-sectional transmission electron microscopy (XTEM) observations were prepared by focus ion beam (FIB) using a FEI Helios NanoLab 600 (FEI Company) operating with a 30 keV Ga ion beam, and finally polished and cleaned at 2 keV – 3 pA to reduce the amount of amorphous materials on the specimen. Conventional and in-situ TEM heating were performed on a Philips CM20FEG operating at 200 kV. The EDX maps and spectra were acquired on the same microscope, which is equipped with a Microanalyzer QUANTAX XFlash detector with a 30 mm^2 active area providing an energy resolution of 127 eV. The EDX quantification was performed using Esprit 1.9 software from Bruker, employing the "Cliff and Lorimer ratio method" for quantifying constituent elements, with an absolute uncertainty of about 3% (molar fraction). High-angle annular dark-field scanning transmission electron microscopy (HAADF-STEM) was acquired on a probe corrected ARM JEM JEOL 200F microscope, operating at 200 kV.

3. Results

3.1 As-deposited GST-225/Ge/GST-225 sandwiched structure

Figure 2 shows a bright field (BF) TEM images and EDX chemical maps of the as-grown structure. The amorphousness of the GST and Ge layers is confirmed as well as the targeted 225 composition of the GST layers. While TEM imaging shows abrupt interfaces, the chemical gradients extracted from EDX extend over about 10 nm in the maps and profiles, what must be taken as the spatial resolution limit resulting from the experimental set up (electron beam probe size, specimen tilt, interfacial roughness and verticality, etc.).

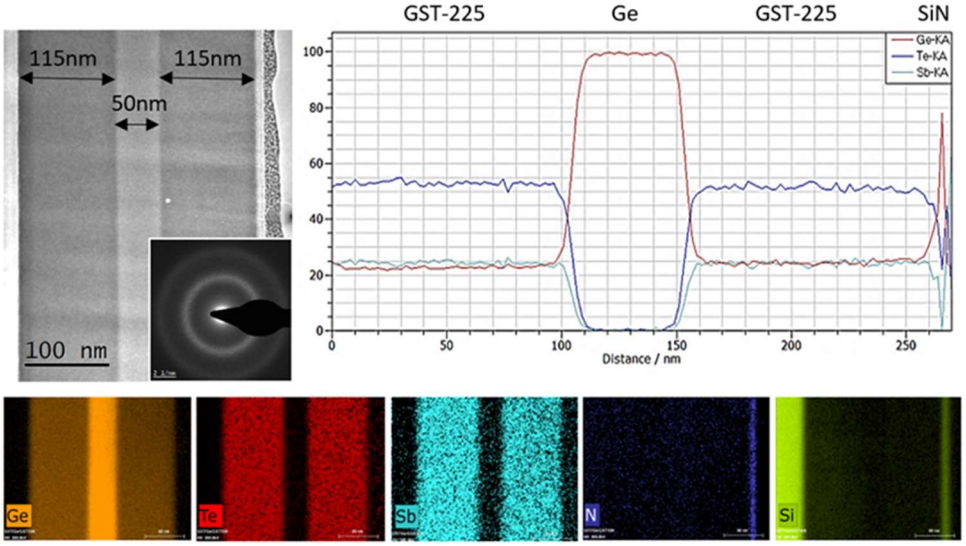

Figure 2*: Top left, BF-TEM image of the initial GST/Ge/GST structure. Top right, composition of the structure as measured by quantitative EDX. The composition of the amorphous GST is 225, as expected. Bottom, EDX chemical maps showing the homogeneity of Ge-Sb-Te distribution.*

3.2 Effect of temperature on Ge diffusion

Firstly, in-situ TEM heating of the specimen has been used to explore the temperatures at which different mechanisms could be activated during thermal annealing. The in-situ heating experiment was performed using a Gatan 652 double tilt heating holder which was connected to a temperature controller and acted as a furnace-type holder. During the annealing, the temperature was increased by steps of 5°C from about 100°C, using a ramping rate of 1°C/s, and held for 5 min at this temperature during which the film was imaged. These observations are summarised in Figure 3.

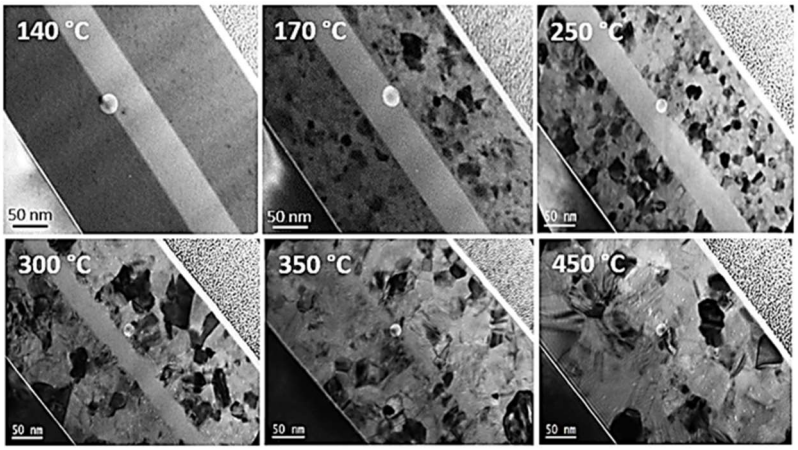

Figure 3*: A series of TEM images extracted from the movie recorded during in-situ annealing. A plot of the heating procedure is shown in the supporting information Figure S1. Further detail of the heating procedure has been presented in the Ref* [32]*.*

In situ TEM heating confirms that the GST layers start to crystallize through homogeneous nucleation in the cubic GST-225 phase from about 140°C. As time passes and the temperature increases, the grains grow in size and coalesce at about 300°C when the cubic grains transit to the stable hexagonal phase. Most importantly, the thickness of the Ge layer (about 50nm) is observed to progressively decrease during annealing, notably from 250°C, and disappears after annealing at 450°C, which shows that Ge diffuses well into the GST layers at these temperatures. In order to identify more precisely the temperatures and times for which Ge diffusion could be demonstrated and studied, we "explored" the result of a panel of thermal anneals, over a wide range of annealing times and temperatures. Figure 4 shows a selection of chemical maps obtained by EDX after ex-situ annealing at different temperatures of the studied structure.

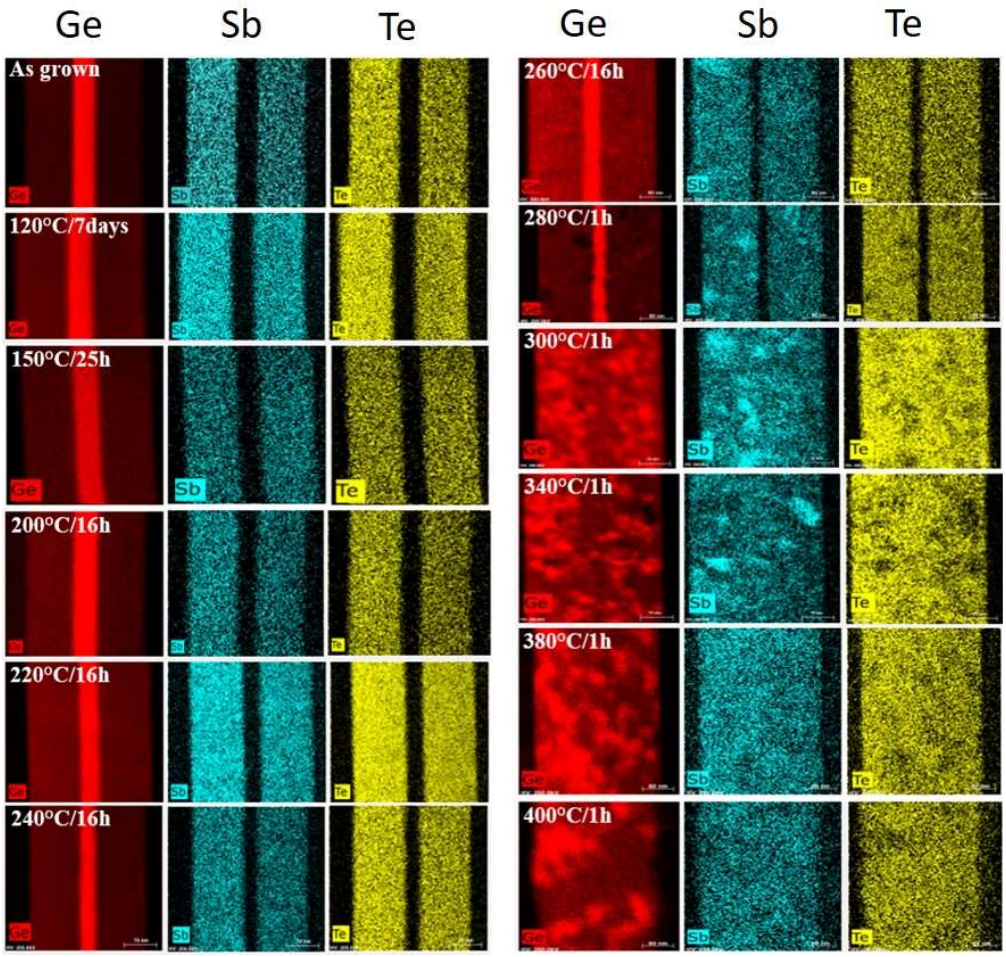

Figure 4: *A series of chemical maps obtained by EDX showing the distribution of Ge, Sb and Te species in the structure after annealing. The GST-225 layers remain homogeneous up to temperatures of around 240°C.*

BF-TEM and STEM-EDX analyses confirm that Ge diffusion can be activated above 200°C. A rapid diffusion occurs at temperatures above or equal to 300°C, for which the Ge layer disappears completely in less than an hour. Strong chemical heterogeneities can then be observed within the GST layers. It is observed that Ge first segregates at the boundaries and junctions of the GST-225 grains, and forms Ge grains. X-ray and selected area electron diffractions (XRD and SAED, respectively) show that these Ge grains develop in the amorphous state and become crystalline only for annealing temperatures equal to or higher than 300°C (shown in SI figure S2,3). Therefore, we have studied in detail the diffusion of Ge at temperatures well below 300°C, allowing the study of Ge diffusion for annealing times of the order of several hours. As a result of all these observations, two temperature ranges were identified as particularly relevant for technology and PCM cells: i) annealing at temperatures below 140°C should allow us to study the possible diffusion of Ge in the amorphous phase, and ii) annealing at 220° for increasing times (isothermal annealing), or for a given (16h) time at temperatures between 200 and 260°C (isochronal annealing) to study Ge diffusion through the GST-225 polycrystalline layer.

3.3 Diffusion in the amorphous phase: annealing at 120°C

Figure 5 shows the results obtained after thermal annealing of the structure for 7 and 13 days at 120°C. After 7 days of annealing, a few grains of cubic GST-225 embedded in the amorphous matrix can be observed. These grains grow for longer annealing times until the layer is fully crystalline after 13 days of annealing.

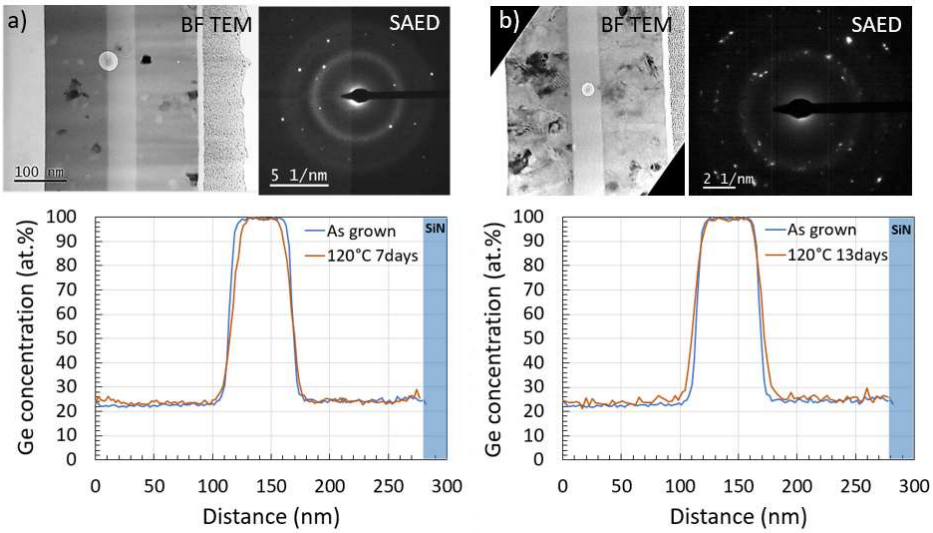

Figure 5*: BF-TEM and SAED images of the layers, and Ge concentration profiles extracted from EDX analysis after annealing at 120°C for 7 days (**a**) and 13 days (**b**).*

The EDX chemical analysis of the structure does not show significant variations in the chemical composition within the layer. The small change in the concentration gradient at the Ge/GST interface can be attributed to small changes in experimental conditions and do not appear significant. This experiment therefore shows that Ge does not redistribute in GST-225 to any significant extent at this low temperature (120°C), both in the amorphous and crystalline phases.

3.4 Diffusion in the crystalline phase

3.4.1 Isothermal annealing at 220°C

Figure 6a shows TEM images of the structure after annealing at 220°C for increasing times. At this temperature, the crystallization of GST-225 is rapid (a few minutes) and the diffusion of Ge therefore takes place mainly through the GST-225 layer in the polycrystalline state. During annealing, the Ge layer becomes thinner and thinner, showing that Ge diffuses into the GST-225 layers. We have measured the variation of the width of the Ge layer over time, which characterizes the Ge “emission” towards the adjacent GST-225 layers. This emission from the source is not constant but decreases with time (shown in Fig. 6b), until it stops at long times. EDX chemical analyses of these layers (Fig. 7) reveal the resulting progressive increase in Ge concentration within the GST-225 layers. This enrichment is of the order of 10% after several days at 220°C.

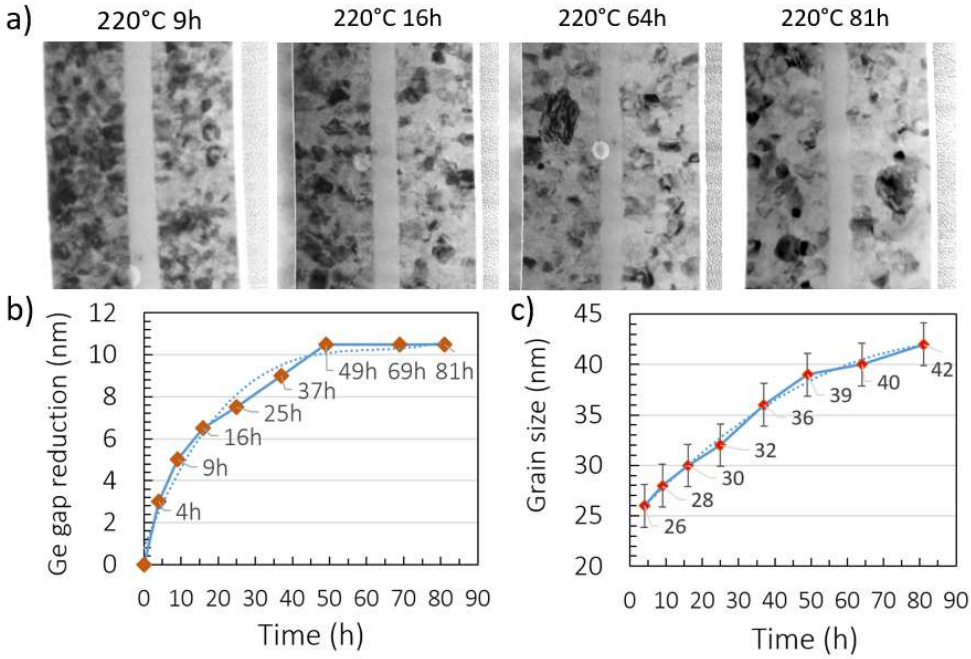

***Figure 6**: **a**) BF-TEM images showing the progressive thinning of the Ge source layer during isothermal annealing at 220°C. **b**) thickness of the Ge layer that diffused into one of the GST-225 layers. **c**) evolution of the average grain size of GST-225 during this annealing.*

Although the concentration gradient at the Ge/GST interface decreases and becomes blunted over time, this reduction remains modest and is not sufficient to explain the strong slowdown of the diffusive transfer of Ge from the source to the GST layers over time. On the other hand, it is important to note that the GST-225 layers mature and that the grains become increasingly larger, almost doubling in size between the beginning and the end of the diffusion experiment (Fig. 6c). High angle annular dark field imaging using scanning TEM (HAADF-STEM), a technique where the contrast is sensitive to the atomic number of the elements, clearly shows that Ge is segregated at the boundaries between the GST-225 grains and grows there over time in the form of grains (see Figure 7). Again, SAED and XRD analyses shown in Figure S2,3 show that Ge remains in amorphous phase both in the source and at the grain boundaries. The fact that the concentration profiles remain flat during annealing evidences that the diffusion is very fast and that the diffusion length involved is very large compared to the thickness of the GST-225 layers. For this reason, classical analysis of the diffusion profiles leading to the extraction of a diffusion coefficient is impossible. It thus seems that the diffusion we are witnessing is a fast diffusion through the grain boundaries, typical of the "C-type diffusion" in Harrison's classification. [29–31] Its slowing down over time must be related to the growth of the GST-225 grains and the reduction of the diffusion paths offered by the grain boundaries. It is also very likely that the stability of the various grain boundaries increases over time, making the interfaces less defective and therefore less likely to support very fast diffusion.

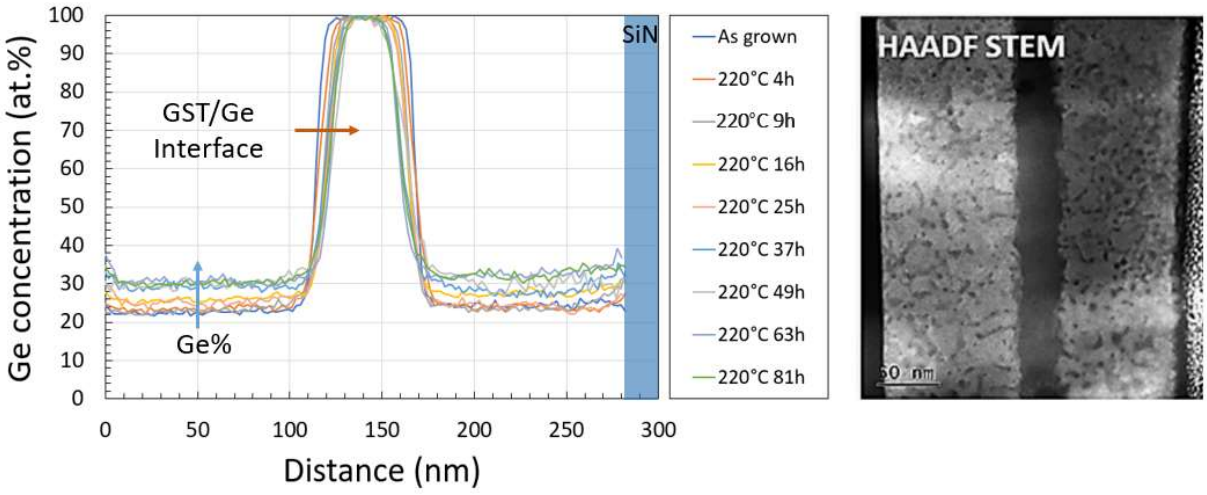

Figure 7: Left, time evolution of the Ge profiles during isothermal annealing at 220°C (extracted from EDX mapping). Right, HAADF STEM image taken on the sample annealed at 220°C for 81h, showing Ge segregation (in black) at the GST-225 grain boundaries and the diffusion paths.

3.4.2 Isochronous annealing of 16h

Figure 8 shows the chemical maps obtained by EDX on the samples after 16h annealing at temperatures between 220 and 260°C as well as the concentration profiles extracted from these maps. It can be seen that, as the temperature increases over this short temperature range, the thickness of the Ge layer dramatically decreases. As a result, the Ge concentration in the GST layers increases up to almost 20%, in excess of the regular 22% stoichiometry of the GST-225 phase. Heterogeneities of composition appear, and betray the formation of amorphous Ge grains within the GST-225 layers, at the grain boundaries.

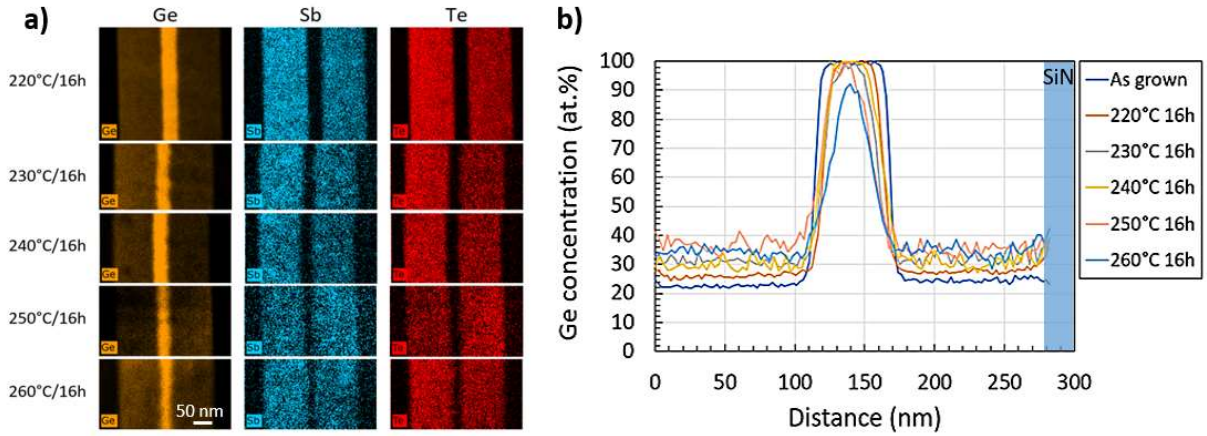

Figure 8: a) Chemical maps (EDX) of the structures annealed 16h at different temperatures and b) Ge-concentration profiles extracted from these maps. At high temperature the signal appears noisy, a consequence of the compositional heterogeneities detected in the images.

It is again important to note that no Ge gradient can be evidenced in the GST layers. The observation of some extension of the gradient over larger distances at the interface between the Ge and GST layers only results from the averaging of the composition at and close to this interface by EDX analysis, while this interface tends to become rough and lose its planarity as it shrinks. These observations show that the mechanisms allowing the emission and diffusion of Ge into the GST-225 polycrystalline layers via the grain boundaries are very strongly activated at these temperatures.

4. Conclusions

Studying the diffusion of an element through a compound containing that same element is complicated. In this work, we have designed a suitable structure to study the thermal diffusion of Ge through the GST-225 alloy. We have studied this diffusion in technologically relevant situations using techniques based on transmission electron microscopy. We have shown that this diffusion could not be evidenced through the amorphous phase of GST, i.e. for temperatures below 140°C beyond which GST-225 crystallizes, even for times of the order of more than ten days. On the other hand, Ge diffusion can be strongly activated at temperatures above 220°C. At these temperatures, this diffusion is very fast and takes place after the crystallization of GST-225 via the boundaries separating the crystalline grains. It follows the "type C" diffusion behaviour as depicted in Harrisson's classification. It corresponds to the situation in which the segregation coefficient is high, which is consistent with the fact that amorphous GGST alloys decompose during annealing. [14–16]

During annealing, Ge diffusion is only limited by the emission of Ge atoms from the solid source and by the density of the diffusion paths available through the polycrystalline solid. This density decreases with time as the GST-225 grains grow in size. However, this rapid diffusion cannot be quantified by the experiments presented in this work because the Ge concentration, while increasing with annealing time, remains independent of the distance to the source. In other words, Ge concentration gradients cannot be demonstrated because the Ge diffusion length ($\sqrt{D.t}$) is much larger than the thickness of the designed GST-225 layer (115nm). However, these results show that diffusion phenomena can affect the chemical composition and morphology of Ge/GST composite materials and thus contribute to the understanding of the resistance drift and loss of integrity which affect the PCMs based on GGST alloys in the SET state, notably at temperatures above 200°C.

Supplementary Materials:

Figure S1 shows the typical heating profile used for in situ TEM experiment. Step jump: 5°C, ramping rate: 1°C/s. Once the set temperature is reached, 5 min of waiting time before observation. Figure S2 shows XRD patterns of samples annealed at 220°C for different time durations. The pink vertical bars represent the expected positions of GST-225 FCC diffraction peaks. The extra peaks at 38° and 44.5° are generated by the substrate on the XRD machine. Figure S3 shows XRD patterns of the as-deposited and annealed samples, at 280°C, 300 and 340°C for 1h. The Ge peak starts to appear only after annealing at 300°C/1h.

Author Contributions: Investigation, writing - review and editing, Minh Anh Luong; Discussion and review the manuscript, Sijia Ran; Sample fabrication, discussion and review the manuscript, Mathieu Bernard; Project administration and funding acquisition, supervision and review manuscript, Alain Claverie. All authors have read and agreed to the published version of the manuscript.

Conflicts of Interest: The authors declare no conflict of interest.

Acknowledgment

This work is part of the "Ô-GST Project" and partially funded by the nano2022 (IPCEI) initiative and by the ST/CNRS Action on GST materials.

References

(1) Burr, G. W.; Breitwisch, M. J.; Franceschini, M.; Garetto, D.; Gopalakrishnan, K.; Jackson, B.; Kurdi, B.; Lam, C.; Lastras, L. A.; Padilla, A.; Rajendran, B.; Raoux, S.; Shenoy, R. S. Phase Change Memory Technology. *Journal of Vacuum Science & Technology B, Nanotechnology and Microelectronics: Materials, Processing, Measurement, and Phenomena* 2010, *28* (2), 223–262. https://doi.org/10.1116/1.3301579.

(2) Wuttig, M.; Yamada, N. Phase-Change Materials for Rewriteable Data Storage. *Nature Mater* 2007, *6* (11), 824–832. https://doi.org/10.1038/nmat2009.

(3) Fong, S. W.; Neumann, C. M.; Wong, H.-S. P. Phase-Change Memory—Towards a Storage-Class Memory. *IEEE Trans. Electron Devices* 2017, *64* (11), 4374–4385. https://doi.org/10.1109/TED.2017.2746342.

(4) Noé, P.; Vallée, C.; Hippert, F.; Fillot, F.; Raty, J.-Y. Phase-Change Materials for Non-Volatile Memory Devices: From Technological Challenges to Materials Science Issues. *Semicond. Sci. Technol.* 2018, *33* (1), 013002. https://doi.org/10.1088/1361-6641/aa7c25.

(5) Guo, P.; Sarangan, A.; Agha, I. A Review of Germanium-Antimony-Telluride Phase Change Materials for Non-Volatile Memories and Optical Modulators. *Applied Sciences* 2019, *9* (3), 530. https://doi.org/10.3390/app9030530.

(6) Arnaud, F.; Zuliani, P.; Reynard, J. P.; Gandolfo, A.; Disegni, F.; Mattavelli, P.; Gomiero, E.; Samanni, G.; Jahan, C.; Berthelon, R.; Weber, O.; Richard, E.; Barral, V.; Villaret, A.; Kohler, S.; Grenier, J. C.; Ranica, R.; Gallon, C.; Souhaite, A.; Ristoiu, D.; Favennec, L.; Caubet, V.; Delmedico, S.; Cherault, N.; Beneyton, R.; Chouteau, S.; Sassoulas, P. O.; Vernhet, A.; Le Friec, Y.; Domengie, F.; Scotti, L.; Pacelli, D.; Ogier, J. L.; Boucard, F.; Lagrasta, S.; Benoit, D.; Clement, L.; Boivin, P.; Ferreira, P.; Annunziata, R.; Cappelletti, P. Truly Innovative 28nm FDSOI Technology for Automotive Micro-Controller Applications Embedding 16MB Phase Change Memory. In *2018 IEEE International Electron Devices Meeting (IEDM)*; IEEE: San Francisco, CA, 2018; p 18.4.1-18.4.4. https://doi.org/10.1109/IEDM.2018.8614595.

(7) Cappelletti, P.; Annunziata, R.; Arnaud, F.; Disegni, F.; Maurelli, A.; Zuliani, P. Phase Change Memory for Automotive Grade Embedded NVM Applications. *J. Phys. D: Appl. Phys.* 2020, *53* (19), 193002. https://doi.org/10.1088/1361-6463/ab71aa.

(8) Ielmini, D.; Wong, H.-S. P. In-Memory Computing with Resistive Switching Devices. *Nat Electron* 2018, *1* (6), 333–343. https://doi.org/10.1038/s41928-018-0092-2.

(9) Islam, R.; Li, H.; Chen, P.-Y.; Wan, W.; Chen, H.-Y.; Gao, B.; Wu, H.; Yu, S.; Saraswat, K.; Philip Wong, H.-S. Device and Materials Requirements for Neuromorphic Computing. *J. Phys. D: Appl. Phys.* 2019, *52* (11), 113001. https://doi.org/10.1088/1361-6463/aaf784.

(10) *Memristive Devices for Brain-Inspired Computing - 1st Edition*. https://www.elsevier.com/books/memristive-devices-for-brain-inspired-computing/spiga/978-0-08-102782-0 (accessed 2021-05-24).

(11) Zuliani, P.; Varesi, E.; Palumbo, E.; Borghi, M.; Tortorelli, I.; Erbetta, D.; Libera, G. D.; Pessina, N.; Gandolfo, A.; Prelini, C.; Ravazzi, L.; Annunziata, R. Overcoming Temperature Limitations in Phase Change Memories With Optimized GexSbyTez. *IEEE Trans. Electron Devices* 2013, *60* (12), 4020–4026. https://doi.org/10.1109/TED.2013.2285403.

(12) Palumbo, E.; Zuliani, P.; Borghi, M.; Annunziata, R. Forming Operation in Ge-Rich GexSbyTez Phase Change Memories. *Solid-State Electronics* 2017, *133*, 38–44. https://doi.org/10.1016/j.sse.2017.03.016.

(13) Privitera, S. M. S.; López García, I.; Bongiorno, C.; Sousa, V.; Cyrille, M. C.; Navarro, G.; Sabbione, C.; Carria, E.; Rimini, E. Crystallization Properties of Melt-Quenched Ge-Rich GeSbTe Thin Films for Phase Change Memory Applications. *Journal of Applied Physics* 2020, *128* (15), 155105. https://doi.org/10.1063/5.0023696.

(14) Luong, M. A.; Agati, M.; Ratel Ramond, N.; Grisolia, J.; Le Friec, Y.; Benoit, D.; Claverie, A. On Some Unique Specificities of Ge-Rich GeSbTe Phase-Change Material Alloys for Nonvolatile Embedded-Memory Applications. *Phys. Status Solidi RRL* 2021, *15* (3), 2000471. https://doi.org/10.1002/pssr.202000471.

(15) Rahier, E.; Ran, S.; Ratel Ramond, N.; Ma, S.; Calmels, L.; Saha, S.; Mocuta, C.; Benoit, D.; Le Friec, Y.; Luong, M. A.; Claverie, A. Crystallization of Ge-Rich GeSbTe Alloys: The Riddle Is Solved. *ACS Appl. Electron. Mater.* 2022, acsaelm.2c00038. https://doi.org/10.1021/acsaelm.2c00038.

(16) Agati, M.; Vallet, M.; Joulié, S.; Benoit, D.; Claverie, A. Chemical Phase Segregation during the Crystallization of Ge-Rich GeSbTe Alloys. *J. Mater. Chem. C* 2019, *7* (28), 8720–8729. https://doi.org/10.1039/C9TC02302J.

(17) Cheng, H. Y.; Hsu, T. H.; Raoux, S.; Wu, J. Y.; Du, P. Y.; Breitwisch, M.; Zhu, Y.; Lai, E. K.; Joseph, E.; Mittal, S.; Cheek, R.; Schrott, A.; Lai, S. C.; Lung, H. L.; Lam, C. A High Performance Phase Change Memory with Fast Switching Speed and High Temperature Retention by Engineering the GexSbyTez Phase Change Material. In *2011 International Electron Devices Meeting*; IEEE: Washington, DC, USA, 2011; p 3.4.1-3.4.4. https://doi.org/10.1109/IEDM.2011.6131481.

(18) Ciocchini, N.; Palumbo, E.; Borghi, M.; Zuliani, P.; Annunziata, R.; Ielmini, D. Modeling Resistance Instabilities of Set and Reset States in Phase Change Memory with Ge-Rich GeSbTe. *IEEE Trans. Electron Devices* 2014, *61* (6), 2136–2144. https://doi.org/10.1109/TED.2014.2313889.

(19) Kim, S.; Burr, G. W.; Kim, W.; Nam, S.-W. Phase-Change Memory Cycling Endurance. *MRS Bull.* 2019, *44* (09), 710–714. https://doi.org/10.1557/mrs.2019.205.

(20) Kiouseloglou, A.; Navarro, G.; Sousa, V.; Persico, A.; Roule, A.; Cabrini, A.; Torelli, G.; Maitrejean, S.; Reimbold, G.; De Salvo, B.; Clermidy, F.; Perniola, L. A Novel Programming Technique to Boost Low-Resistance State Performance in Ge-Rich GST Phase Change Memory. *IEEE Trans. Electron Devices* 2014, *61* (5), 1246–1254. https://doi.org/10.1109/TED.2014.2310497.

(21) Prazakova, L.; Nolot, E.; Martinez, E.; Fillot, F.; Rouchon, D.; Rochat, N.; Bernard, M.; Sabbione, C.; Morel, D.; Bernier, N.; Grenier, A.; Papon, A.-M.; Cyrille, M.-C.; Navarro, G. Temperature Driven Structural Evolution of Ge-Rich GeSbTe Alloys and Role of N-Doping. *Journal of Applied Physics* 2020, *128* (21), 215102. https://doi.org/10.1063/5.0027734.

(22) Mitrofanov, K. V.; Kolobov, A. V.; Fons, P.; Wang, X.; Tominaga, J.; Tamenori, Y.; Uruga, T.; Ciocchini, N.; Ielmini, D. Ge L_3 -Edge X-Ray Absorption near-Edge Structure Study of Structural Changes Accompanying Conductivity Drift in the Amorphous Phase of $Ge_2Sb_2Te_5$. *Journal of Applied Physics* 2014, *115* (17), 173501. https://doi.org/10.1063/1.4874415.

(23) Singh, M. K.; Ghosh, C.; Miller, B.; Kotula, P. G.; Tripathi, S.; Watt, J.; Bakan, G.; Silva, H.; Carter, C. B. *In Situ* TEM Study of Crystallization and Chemical Changes in an Oxidized Uncapped $Ge_2Sb_2Te_5$ Film. *Journal of Applied Physics* 2020, *128* (12), 124505. https://doi.org/10.1063/5.0023761.

(24) Privitera, S. M. S.; Sousa, V.; Bongiorno, C.; Navarro, G.; Sabbione, C.; Carria, E.; Rimini, E. Atomic Diffusion in Laser Irradiated Ge Rich GeSbTe Thin Films for Phase Change Memory Applications. *J. Phys. D: Appl. Phys.* 2018, *51* (14), 145103. https://doi.org/10.1088/1361-6463/aab1d0.

(25) J. Akola; R. O. Jones. *Structural Patterns in GeSbTe Phase-Change Materials*. NIC Symposium 2008, G. M¨unster, D. Wolf, M. Kremer (Editors), John von Neumann Institute for Computing, J¨ulich, NIC Series, Vol. 39, ISBN 978-3-9810843-5-1, pp. 169-176, 2008. (accessed 2022-03-23).

(26) Li, T.; Shen, J.; Wu, L.; Song, Z.; Lv, S.; Cai, D.; Zhang, S.; Guo, T.; Song, S.; Zhu, M. Atomic-Scale Observation of Carbon Distribution in High-Performance Carbon-Doped $Ge_2Sb_2Te_5$ and Its Influence on Crystallization Behavior. *J. Phys. Chem. C* 2019, *123* (21), 13377–13384. https://doi.org/10.1021/acs.jpcc.9b02098.

(27) Shen, J.; Li, T.; Chen, X.; Jia, S.; Lv, S.; Li, L.; Song, Z.; Zhu, M. Dynamic Evolution of Thermally Induced Element Distribution in Nitrogen Modified Phase Change Materials. *Journal of Applied Physics* 2020, *128* (7), 075701. https://doi.org/10.1063/5.0006519.

(28) Novielli, G.; Ghetti, A.; Varesi, E.; Mauri, A.; Sacco, R. Atomic Migration in Phase Change Materials. In *2013 IEEE International Electron Devices Meeting*; IEEE: Washington, DC, USA, 2013; p 22.3.1-22.3.4. https://doi.org/10.1109/IEDM.2013.6724683.

(29) Peterson, N. L. Grain-Boundary Diffusion in Metals. *International Metals Reviews* 1983, *28* (1), 65–91. https://doi.org/10.1179/imtr.1983.28.1.65.

(30) Sommer, J.; Herzig, Chr. Direct Determination of Grain-boundary and Dislocation Self-diffusion Coefficients in Silver from Experiments in Type-C Kinetics. *Journal of Applied Physics* 1992, *72* (7), 2758–2766. https://doi.org/10.1063/1.352328.

(31) Mehrer, H. *Diffusion in Solids*; Cardona, M., Fulde, P., von Klitzing, K., Queisser, H.-J., Merlin, R., Störmer, H., Series Eds.; Springer Series in Solid-State Sciences; Springer Berlin Heidelberg: Berlin, Heidelberg, 2007; Vol. 155. https://doi.org/10.1007/978-3-540-71488-0.

(32) Luong, M.; Cherkashin, N.; Pecassou, B.; Sabbione, C.; Mazen, F.; Claverie, A. Effect of Nitrogen Doping on the Crystallization Kinetics of Ge2Sb2Te5. *Nanomaterials* 2021, *11* (7), 1729. https://doi.org/10.3390/nano11071729.